



1 Interactive coupling of a Greenland ice sheet model in NorESM2

2 Heiko Goelzer¹, Petra M. Langebroek¹, Andreas Born², Stefan Hofer^{3,4}, Konstanze Haubner², Michele
3 Petrini¹, Gunter Leguy⁵, William H. Lipscomb⁵, Katherine Thayer-Calder⁵

4 ¹NORCE Norwegian Research Centre, Bjerknes Centre for Climate Research, Bergen, Norway

5 ²Department of Earth Science, University of Bergen, Bjerknes Centre for Climate Research, Bergen, Norway

6 ³School of Geographical Sciences, University of Bristol, Bristol, UK

7 ⁴Department of Geosciences, University of Oslo, Oslo, Norway

8 ⁵Climate and Global Dynamics Laboratory, NSF National Center for Atmospheric Research, Boulder, CO, USA

9
10 *Correspondence to:* Heiko Goelzer (heig@norceresearch.no)

11 Abstract

12 On the backdrop of observed accelerating ice sheet mass loss over the last few decades, there is growing
13 interest in the role of ice sheet changes in global climate projections. In this regard, we have coupled the
14 Norwegian Earth System Model (NorESM) with the Community Ice Sheet Model (CISM) and have
15 produced an initial set of climate projections including an interactive coupling with a dynamic Greenland
16 ice sheet. Our focus in this manuscript is the description of the coupling, the model setup and the
17 initialisation procedure. To illustrate the effect of the coupling, we have further performed one chain of
18 experiments under historical forcing and subsequently under high future greenhouse gas forcing (SSP5-
19 8.5) until 2100 and extended until 2300. We find a limited impact of the dynamical ice sheet changes on
20 the global response of the coupled model under the given forcing and experimental setup when comparing
21 to a standard CMIP6 simulation of NorESM with a fixed ice sheet.

22 1 Introduction

23 Ice sheets are regularly discussed and studied in the context of their future sea-level contribution (Seroussi
24 et al., 2020; 2024; Goelzer et al., 2020) and as potential tipping elements in the Earth system (e.g., Pattyn
25 et al., 2018). However, ice sheets are recognised not only as Earth system components that strongly
26 respond to climate changes, but also for their potential to influence climate in turn through interactions
27 with atmosphere, land and ocean (e.g. Vizcaino, 2014). Studying ice sheet - climate interactions therefore
28 requires the ice sheets to be coupled to the other Earth system components. These feedbacks become
29 relevant on long enough timescales, typically centennial to multi-millennial. Relevant large-scale
30 processes that give rise to feedbacks include the influence of a changing ice sheet topography on surface
31 temperature and atmospheric circulation (Merz et al., 2014; 2016), changes in runoff and iceberg fluxes
32 that modify ocean stratification (Martin & Biastoch, 2023) and circulation, and ice sheet expansion or
33 retreat that change the planetary albedo and the potential for vegetation, modifying the radiation and
34 surface energy budget (Vizcaino et al., 2010; Stone and Lunt, 2013).



35 Given the long timescales on which some of these interactions manifest, modelling climate–ice sheet
36 interactions has until recently been mostly out of reach for high-complexity, high-resolution Coupled
37 Model Intercomparison Project (CMIP) models, with CESM2 and UKESM being the only models that
38 delivered coupled climate-ice sheet simulation results under CMIP6 (Muntjewerf et al., 2021; Smith et
39 al., 2021). A large body of work has also focussed on models of lower complexity and/or lower resolution
40 to advance coupled climate–ice sheet science over the last two decades (e.g., Huybrechts et al., 2002;
41 Ridley et al., 2005; Mikolajewicz et al., 2007; Ganopolski et al., 2010; Goelzer et al., 2011; Roche et al.,
42 2014; Gregory et al., 2020). The challenge inherent in these simulations from the ice sheet perspective is
43 bridging the gap between climate boundary conditions produced at a spatial resolution of up to several
44 degrees to the finer ice sheet scale (typical resolution of only a few km). In addition, climate biases often
45 translate into biases in ice sheet state, which has been mitigated e.g. by use of anomaly methods or ad-
46 hoc corrections (e.g. Goelzer et al., 2012). While these problems are typically reduced with higher
47 resolution and lower biases, they remain some of the most important challenges when implementing ice
48 sheet dynamics in climate models. A key advance, paving the way to include ice sheets eventually in
49 CMIP-type climate models, was the advent of efficient downscaling procedures (Vizcaino et al., 2010;
50 2013; 2014; Sellevold et al., 2019), that produce relatively high-quality surface mass balance (SMB) as
51 ice sheet forcing. These exploit a strong elevation (temperature) dependence of some surface mass and
52 energy balance components, in particular of the melt process, which is why they were first successfully
53 implemented for simulations including the Greenland ice sheet (GrIS). For the significantly colder
54 Antarctic ice sheet at present, the SMB is dominated by the distribution of snowfall, which is notoriously
55 difficult to downscale and hinges on the native resolution of atmospheric dynamics. Another remaining
56 challenge for coupled modelling are how to treat the interaction of ice sheets and ocean for the narrow
57 fjords of Greenland and the ice shelves in Antarctica, that are equally not resolved in global climate
58 models. Furthermore, initialising the climate-ice sheet system is a difficult task due to the specific
59 response timescales of the different systems. There is a strong interest of many modelling groups
60 worldwide to overcome these challenges and to work towards coupled climate–ice sheet simulations
61 leading up to CMIP7. These coupled simulations are supported by a community effort under the Ice Sheet
62 Model Intercomparison Project (ISMIP7).

63
64 In this paper, we describe the implementation and first results of GrIS coupling in the Norwegian Earth
65 System Model (NorESM), which builds on a similar development for CESM2 and the Community Ice
66 Sheet Model (CISM, Lipscomb et al., 2019). We describe the model with focus on climate–ice sheet
67 interactions and initialisation (Sect. 2) and the experimental setup (Sect. 3). We show results in section 4
68 and close with Discussions (Sect. 5) and Conclusions (Sect. 6).

69 **2 Model description**

70 In this section, we describe our novel coupled modelling framework consisting of climate and ice sheet
71 components, the dynamic coupling and the initialisation procedure.



72 **2.1 The Norwegian Earth System model (NorESM)**

73 NorESM is a full-complexity CMIP-type Earth system model (ESM) mainly developed by the Norwegian
74 Climate Centre (NCC) consortium. Here, we discuss the model version NorESM2 (Seland et al., 2020),
75 which contributed to CMIP6 (Eyring et al., 2016) without dynamic ice sheets (NorESM2fixed). We have
76 expanded from this CMIP6 version and included interactive coupling with a dynamic GrIS component
77 (Sect. 2.2). NorESM2 shares many technical features with CESM2 (Danabasoglu et al., 2020) because
78 the fundamental model components for land (CLM), atmosphere (CAM), sea ice (CICE), and land ice
79 (CISM) are the same (Fig. 1). The coupling interface between the ice sheet on the one hand and atmosphere
80 and land models on the other hand is also inherited from CESM2, using the same elevation-class approach
81 (Sec 2.3) to provide surface mass and energy balance from the atmosphere (CAM) via the land model
82 (CLM) to the ice sheet model. The ocean model in NorESM2 (BLOM), the ocean biogeochemical
83 component (iHAMOCC) and extended atmospheric chemistry options (in CAM) are distinguishing
84 features and lead to a different climate sensitivity compared to CESM2— specifically, a lower transient
85 climate response (Seland et al., 2020). In version 2, NorESM can run with only one interactive ice sheet
86 domain at a time (here Greenland). Implementing an Antarctic ice sheet and paleo ice sheets are subject
87 to future model development.

88 We have run coupled climate-ice sheet simulations with NorESM2 at two different horizontal resolutions
89 of the atmosphere model, called NorESM2-MM ($1^\circ \times 1^\circ$) and NorESM2-LM ($2^\circ \times 2^\circ$ resolution) that
90 have both uncoupled (NorESM2fixed) contributions to CMIP6 to compare to. In the following we focus
91 mainly on the higher resolution version and use the name NorESM2 for NorESM2-MM unless indicated
92 otherwise.

93 **2.2 The Community Ice Sheet Model (CISM)**

94 CISM is a thermodynamically-coupled ice sheet model (Lipscomb et al., 2019), run on a structured grid,
95 that can be used for both coupled (Muntjewerf et al., 2020a; b; Petrini et al., 2024) and standalone
96 applications (Lipscomb et al., 2021; Berdahl et al., 2023; Rahlves et al., 2024).

97 As the GrIS component in NorESM2, we use CISM at 4×4 km horizontal resolution and with 11 unequally
98 spaced vertical levels on a variable-thickness sigma coordinate. The ice sheet domain is laid out on a
99 standard polar stereographic projection and restricted to the main Greenland island. The momentum
00 balance is solved with the higher-order depth integrated viscosity approximation (DIVA) approach
01 (Goldberg, 2011; Robinson et al., 2022) including longitudinal stress transmission in a computationally
02 efficient vertically averaged setup. We use a basal sliding law following Schoof et al. (2005) with the
03 option to locally calibrate basal friction coefficients (Lipscomb et al., 2021) that we exploit in the
04 initialisation approach described in Sect. 2.4. Bedrock change due to glacial isostatic adjustment is not
05 activated. The basic ice sheet model configuration is similar to the NSF NCAR-CISM contribution to the
06 ISMIP6 (Nowicki et al., 2020) standalone projections (Goelzer et al., 2020).



07 2.3 Coupled Climate - Ice Sheet interactions

08 Surface energy balance and surface mass balance

09 In NorESM2, glacier and ice sheet surfaces are treated as an additional land surface type of the land model
10 CLM. This implies that the surface energy and mass balance are computed by the land model, which
11 passes the surface mass balance (SMB) and ice surface temperature as a forcing to CISM once a year.
12 The SMB is calculated as the difference between accumulation (snowfall and refreezing of rainfall and/or
13 previously melted snow within the snowpack) and ice loss from surface melt and sublimation:

$$15 \text{ SMB} = \text{Snowfall} + \text{Refreezing} - \text{Melt} - \text{Sublimation}.$$

16
17 The available energy to melt snow and ice is calculated from the sum of net surface radiation, latent and
18 sensible turbulent heat fluxes, and ground heat fluxes at the atmosphere/land interface over glaciated grid
19 cells (Lawrence et al., 2019). The influence of elevation on both surface melt energy and SMB (Hermann
20 et al., 2018; Van de Wal et al., 2012) poses a challenge in bridging between the relatively low horizontal
21 resolution in CLM (here 1° or 2°) and the higher CISM horizontal resolution (here 4 km). This is
22 particularly true at the ice sheet margins, where resolving steep SMB gradients becomes difficult at coarse
23 resolution. CLM addresses this challenge by calculating the SMB at multiple elevation classes (ECs)
24 which allows to account for subgrid-scale elevation variations over glaciated land units (Lipscomb et al.,
25 2013; Vizcaino et al., 2014; Sellevold et al., 2019; Muntjewerf et al., 2021). To encompass the full range
26 of CISM grid surface elevations while adequately representing subgrid-scale topographic variations, ten
27 ECs are considered with boundaries at 0, 200, 400, 700, 1,000, 1,300, 1,600, 2,000, 2,500, 3,000, and
28 10,000 m (Muntjewerf et al., 2021, Petrini et al., 2023). The choice of this non-uniform boundary
29 distribution is explained by the larger number of ECs needed to capture the steep lower topography at the
30 ice sheet margins, as opposed to a relatively flat high-elevation terrain in the ice sheet interior (Sellevold
31 et al., 2019). In each EC, surface energy fluxes and their impact on SMB are calculated independently.
32 First, the CLM grid cell near-surface temperature (corresponding to the CLM mean grid cell elevation) is
33 adjusted to the ‘virtual’ elevation in each EC using a uniform lapse rate of -6 °K/km. The temperature in
34 each EC is then used to calculate EC-specific potential temperature, specific humidity, air density, and
35 surface pressure, assuming vertically uniform relative humidity. The CLM grid cell precipitation does not
36 vary through ECs but is partitioned into snow or rain based on the elevation-corrected near-surface
37 temperature in each EC. If the downscaled temperature is below -2°C, precipitation is assumed to be
38 100% snow, whereas for temperatures above 0°C it is considered as 100% rain. For intermediate
39 temperatures between -2 and 0 °C, a linear interpolation is applied to determine the rain-to-snow ratio
40 (Muntjewerf et al., 2021). Snowfall is converted to ice when the depth of the snowpack exceeds a
41 threshold of 10 m water equivalent, whereas for lower snowpack depth, the accumulated snow does not
42 directly contribute to the SMB. Liquid and solid precipitation and the EC-specific interpolated fields are
43 used to calculate the SMB in each EC. After this calculation, the SMB is downscaled to the higher-
44 resolution CISM domain through a horizontal bilinear interpolation and a linear vertical interpolation
45 between ECs adjacent to the CISM grid cell elevation. Following these interpolations, the discrepancy
46 between total mass accumulation and loss in the source (CLM) and destination (CISM) grids is calculated,



47 and two different normalisation factors (one for the accumulation region, and one for the ablation region)
48 are applied to achieve mass conservation. The CLM near-surface temperature is remapped from CLM to
49 CISM using the same EC method, with the only difference being that no normalisation factor is applied
50 after the downscaling. More details on the coupling between CLM and CISM and on the ECs methods
51 can be found in Muntjewerf et al. (2021) and Sellevold et al. (2019).

52 In the results section below, we will compare the output of this EC approach implemented in NorESM
53 (NorESM2-EC) over the historical period with two different results from the regional climate model MAR
54 v3.12. In one case the output is produced by forcing MAR with lateral boundary conditions from the
55 CMIP6 version of NorESM2-MM (NorESM2-MAR). Note that this version of NorESM2 does not
56 include an interactive ice sheet model and represents a different ensemble member with different inter-
57 annual and inter-decadal variability. In the other case, MAR is forced with lateral boundary conditions
58 coming from the reanalysis data set ERA5 (ERA5-MAR).

59 **Ice sheet surface topography**

60 To include the impact of changing ice sheet surface topography on atmospheric circulation, we adopt an
61 asynchronous procedure that modifies the restart files of the atmospheric model (Lofverstrom et al.,
62 2020). Topographic changes on the GrIS domain are interpolated and incorporated in the high-resolution
63 input dataset for the atmospheric component (CAM). Surface topography and surface roughness are then
64 re-calculated and written into the CAM restart file. The procedure is time-consuming and model progress
65 is paused during the update. Including the update at runtime instead would be desirable but requires
66 substantial recoding of the way topography and roughness boundary conditions are currently handled in
67 CAM. In the present experiments we update the topography every five years, in line with the restart
68 checkpoint frequency in our model runs and with earlier experiments with CESM2 (Muntjewerf et al.,
69 2021).

70

71 **Melt and freshwater fluxes**

72 As described above, the ice sheet surface is treated as an additional surface type in the land model, and
73 surface mass and energy calculations are handled by CLM. Surface meltwater runoff is consequently also
74 handled by CLM and routed to the ocean through the runoff scheme (MOSART). This liquid runoff is
75 coupled on hourly timescales at the time resolution of the land model. Ice sheet calving fluxes (i.e., solid
76 ice discharge) are converted to freshwater and passed directly to the ocean, where the energy needed to
77 melt ice is taken from the ocean heat reservoir. Solid ice fluxes are cumulated and passed to the ocean
78 annually.

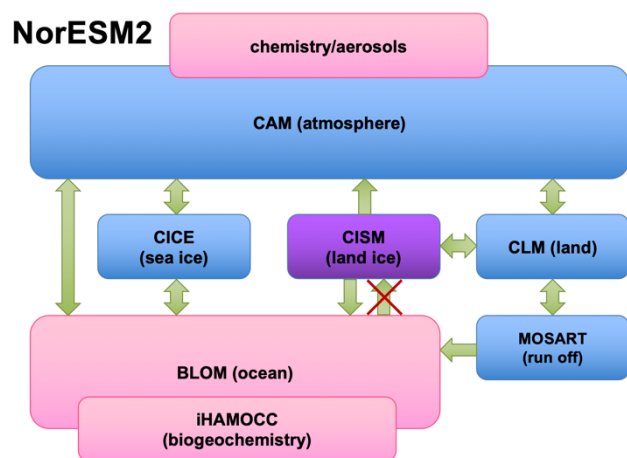
79

80 **Ice–ocean interactions**

81 Our model does not include direct effects of the ocean on the ice sheet (e.g., via ocean temperature or
82 salinity). Also, the ice sheet model is restricted to simulating grounded ice, with all floating ice removed
83 immediately. The spatial scale of narrow marine-terminating outlet glaciers around Greenland is on the



84 order of only a few kilometres, while a typical horizontal resolution of the ocean model is on the order of
 85 100 km (here at $1^\circ \times 1^\circ$). Resolving their interactions is therefore challenging. Complex interactions
 86 between the outflowing glacial meltwater, inflowing ocean water, sea-ice and icebergs and variations in
 87 local bathymetry and glacier geometry in ~ 200 individual fjords complicate the situation. Feasible
 88 approaches are currently mostly found in simple parameterisations describing the impact of the ocean on
 89 the ice sheet (e.g., Slater et al., 2019; 2020). In the absence of dedicated oceanic forcing of the marine-
 90 terminating outlet glaciers in our model, glaciers are simulated to respond passively to changes in inland
 91 inflow and SMB and deliver excess mass to the ocean (e.g. Muntjewerf et al., 2020a; b).
 92



93

94 **Figure 1. NorESM2 model components**

95

96 **2.4 Initialisation**

97 The aim of our initialisation approach is to produce a pre-industrial coupled model configuration (for
 98 simplicity represented by year 1850), that is close to steady state for the climate and ice sheet components.
 99 In this first coupled setup with NorESM2, we achieve that by initialising the ice sheet as close as possible
 00 to the observed present-day configuration, under SMB forcing derived from a pre-industrial simulation
 01 of NorESM2 without ice sheet coupling (NorESM2fixed). The arguments for admitting this slight
 02 inconsistency (pre-industrial forcing vs present-day ice sheet configuration) are that i) we do not know
 03 the precise ice sheet geometry before the start of routine satellite observations in ~ 1990 , ii) differences
 04 between the pre-industrial and present-day ice sheet are likely small compared to what can be resolved
 05 by the atmospheric component and iii) the climate components in NorESM2fixed have had the present-
 06 day ice sheet geometry as topographic boundary condition in all experiments, including the pre-industrial.
 07 Furthermore, this approach facilitates the setup and reduces the preparation time of the coupled model, as
 08 it can be used with the tuning of an existing NorESM2fixed configuration from CMIP6.

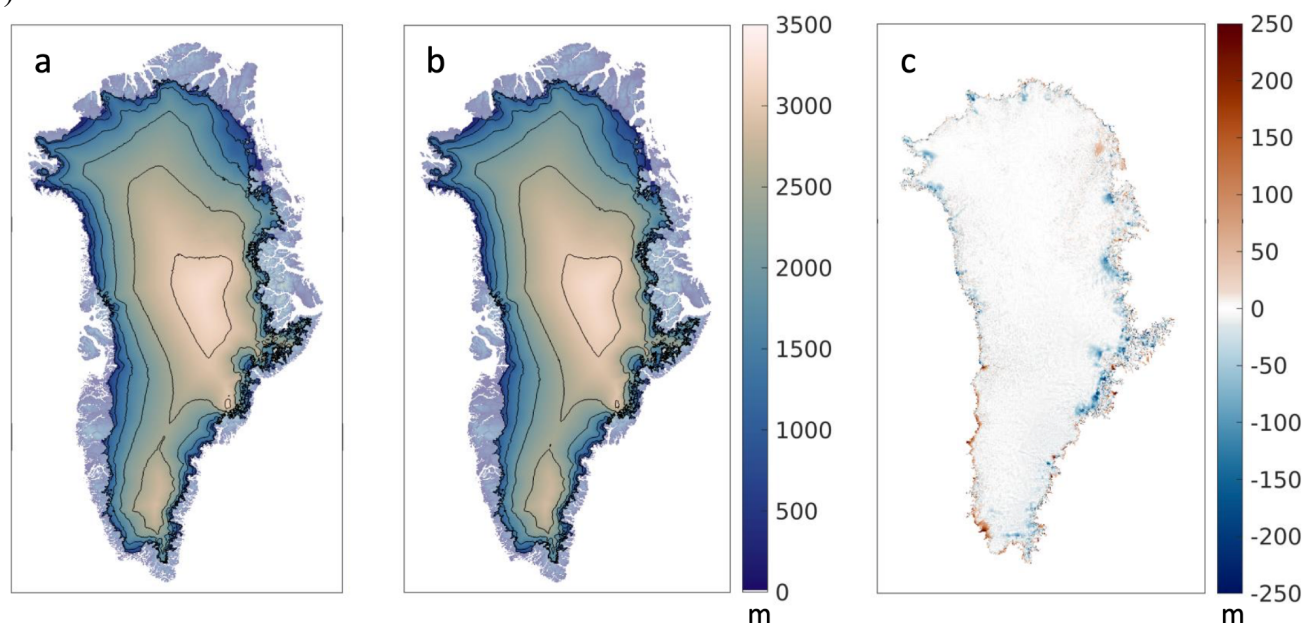


09

2.4.1 Ice sheet model initialisation

10 For the coupled experiments, our method leans on our experience with standalone ice sheet simulations
11 (e.g., Goelzer et al., 2020; Rahlves et al., 2024) and attempts to minimise the initial drift arising from
12 introducing the ice sheet component into the global model. To that end we have calibrated the basal
13 friction parameters (Lipscomb et al., 2019) of the ice sheet model to closely reproduce the present-day
14 observed ice sheet elevation when forced with output from NorESM2fixed over the pre-industrial period.
15 We also use three options implemented in CISM that control the behaviour of ice at the margins: 1) an
16 option to remove ice caps and glaciers in the periphery that are not connected to the main ice sheet (option
17 ‘remove_ice_caps’); 2) the ice sheet is constrained by masking to the observed ice extent, allowing for
18 retreat but not expansion of the ice sheet area beyond the present-day margins (option ‘force_retreat’ with
19 constant mask); 3) Ice is not allowed to form in locations disconnected from the main ice sheet (option
20 ‘block_inception’). This means that new ice sheet cells can only form by flow from an already existing
21 cell. In all three cases, ice thickness is set to zero and ice mass is removed as calving flux. These
22 constraints are justified for forcing scenarios where we expect an ice sheet extent similar or retreated
23 compared to today (historical and future periods). In other cases, e.g. glacial periods, this approach should
24 be modified.

25 In combination, masking and calibration of the basal friction parameters are means to practically deal
26 with the climatic biases in NorESM2 and the limitations of the ice sheet model. The dynamic behaviour
27 of the model is somewhat impacted by these choices (e.g. Berends et al., 2023), but the result is an overall
28 better agreement with the ice sheet surface elevation to which the climate model is already relaxed (Fig.
29 2).



30
31
32

Figure 2. Ice sheet surface elevation. a) Target surface elevation based on present-day observations. b) Ice sheet model surface elevation after initialisation for year 1850. c) Difference in surface elevation on the modelled ice mask.



33 2.4.2 Coupled model initialisation

34 The desired consequence of the modelling decisions described in the last section is to minimise model
 35 drift and rapidly reach a quasi-equilibrium for the coupled system with an ice sheet geometry close to
 36 observed. It has allowed us to perform coupled simulations with very limited model drift after a short
 37 relaxation of only 50 years (c1850 in Table 1). This is a strong benefit over other approaches that require
 38 relatively expensive iterations to bring the ice sheet and climate states into agreement (e.g., Fyke et al.,
 39 2014; Lofverstrom et al., 2020; Muntjewerf et al., 2020a; b). A slight increase in precipitation over
 40 Greenland margins in response to the coupling observed during preliminary tests was further compensated
 41 by initialising the ice sheet to a slightly biased surface mass balance forcing. Instead of calculating the
 42 long-term mean SMB from the last 50 years of a pre-industrial steady state experiment of NorESM2fixed,
 43 we use only the 25 years with the highest SMB for the improved initialisation. As opposed to a slight
 44 mass gain in the preliminary forward experiment, the result is a small overall ice sheet mass loss, as the
 45 ice sheet relaxes to the ensuing lower SMB in the forward experiment (Fig. 3d).

46 3 Experimental setup

47 We have performed one chain of experiments (Table 1) that follow a subset of the protocol for coupled
 48 climate–ice sheet simulations (Nowicki et al., 2016) of the Ice Sheet Model Intercomparison Project for
 49 CMIP6 (ISMIP6). The first coupled experiment (c1850) is a 50-year relaxation in which the climate and
 50 ice sheet are first brought together after separate initialisation. Following is a standard historical
 51 experiment (cHIST) from 1850–2014, and a projection under forcing scenario SSP5-8.5 to 2100
 52 (cSSP585), that is further prolonged with a scenarioMIP extension (O'Neill et al., 2016) for SSP5-8.5 to
 53 2300 (cSSP585Ext). We also performed a control experiment continuing the standard CMIP6 pre-
 54 industrial experiment for 350 years (cControl). For all coupled experiments, we compare to results from
 55 uncoupled experiments (NorESM2fixed, climate simulations indicated with “n”, Table 1) to evaluate the
 56 impact of the coupling, albeit with only one ensemble member per model setup.

57
 58 **Table 1. Experiment overview.**

Coupled experiments (c)	Uncoupled experiments (n)	Time	Comment
-	n1850 (NorESM2fixed)	50 years	Standard CMIP6 pre-industrial experiment
-	ISM spinup	5000 years	Standalone ice sheet spinup to NorESM2 SMB
c1850	n1850	50 years	Spinup (or coupled initialisation)
cHIST	nHIST	1850 – 2014	Historical experiment
cSSP585	nSSP585	2015 – 2100	Projection
cSSP585Ext	nSSP585Ext	2101 – 2300	ScenarioMIP prolongation *
cControl	nControl	350 years	Control experiment under preindustrial forcing

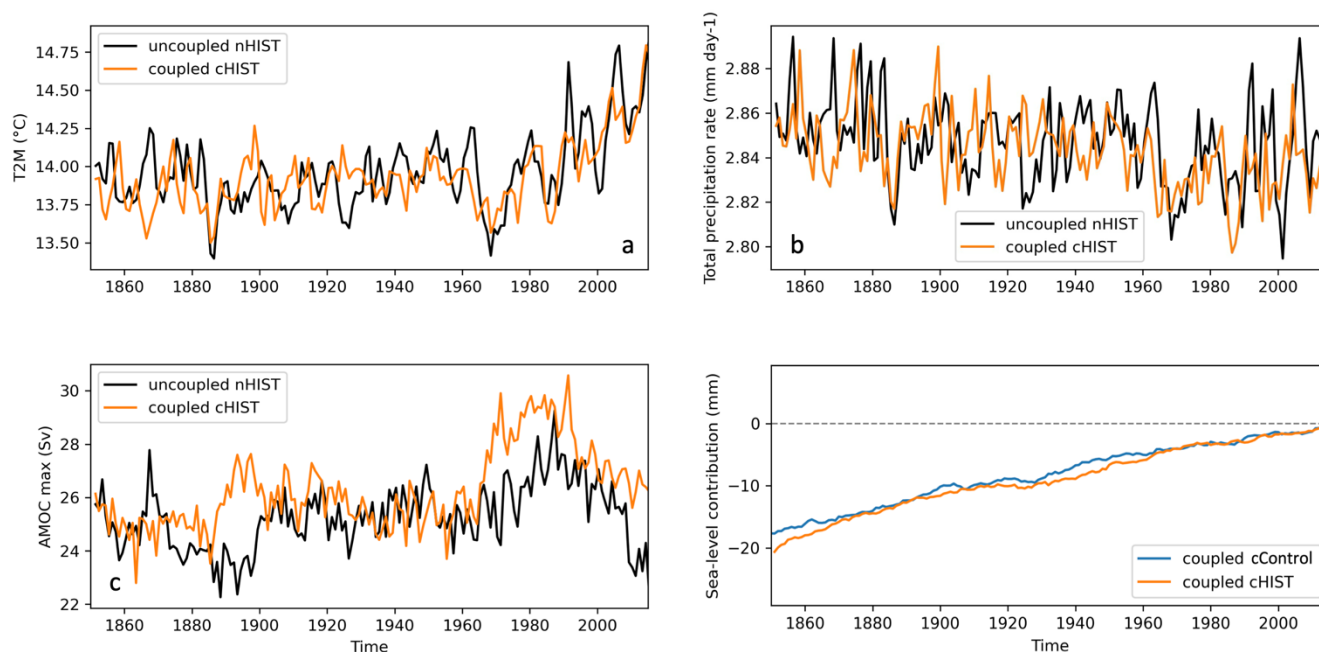


59 * SSP585Ext extends SSP585 to year 2300 with CO₂ emissions that are reduced linearly starting in
 60 2100 to less than 10 GtC yr⁻¹ in 2250 and constant during the last 50 years. Other emissions are held
 61 constant at 2100 levels.
 62

63 4 Results

64 4.1 Simulation over the historical period

65 Over the historical period, coupled and uncoupled experiments show overall a similar mean climate
 66 evolution (Fig. 3a-c). There are differences between the phasing of their interannual and inter-decadal
 67 variability, but this is to be expected in freely evolving (i.e., not nudged to observations) ESM simulations.
 68 The ice sheet exhibits a small mass loss (positive sea-level contribution) of similar magnitude in the
 69 historical experiment cHIST and the control experiment cControl (Fig. 3d), as a result of the initialisation
 70 to slightly biased SMB forcing described above (Sect. 2.4.2). The overall mass loss rate over the historical
 71 period is comparable to reconstructions (Zuo and Oerlemans, 1997; Box and Colgan, 2013), while
 72 episodes of readvance and retreat suggested e.g. by Bjørk et al. (2012) are not captured.
 73



74 **Figure 3. Climate and ice sheet evolution over the historical period. Coupled (orange) and uncoupled (black) evolution of a) two-**
 75 **meter air temperature (T2M), b) total precipitation rate c) Atlantic meridional overturning circulation (AMOC). d) sea-level**
 76 **contribution from the GrIS for coupled experiments cHIST (orange) and cControl (blue).**
 77

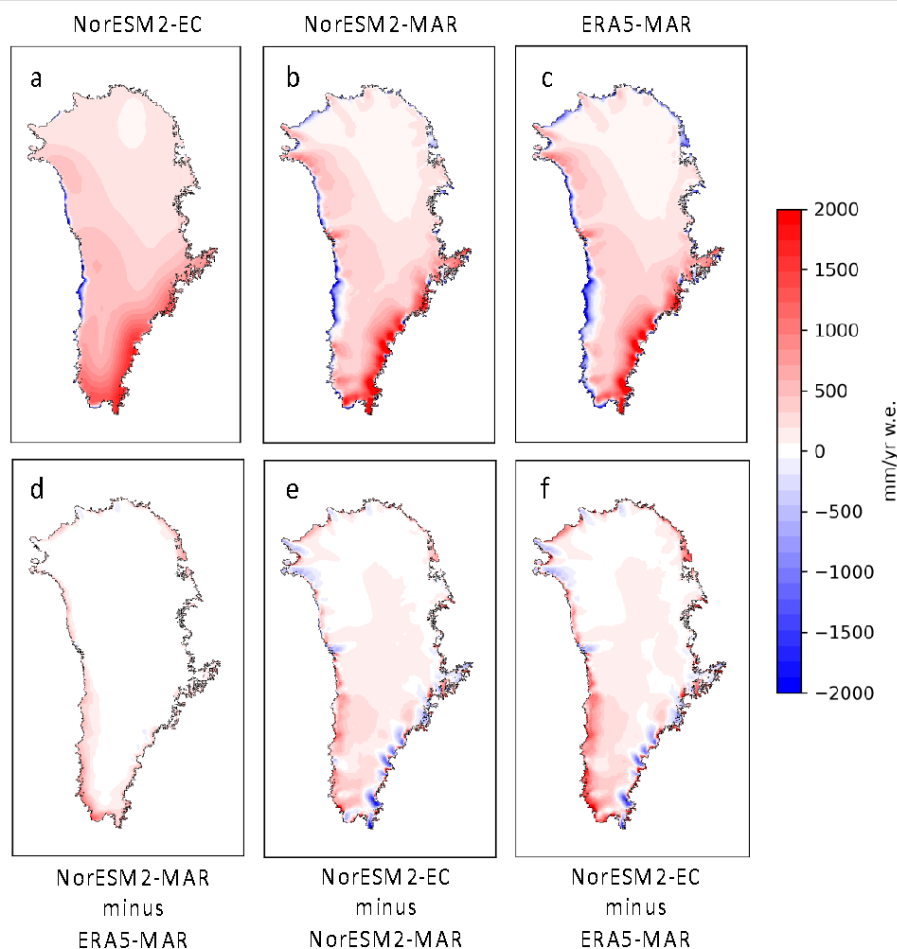
78



79 **4.2 SMB evaluation over the reanalysis period**

80 Figure 4 shows the mean SMB over the period 1960-1989 as simulated directly by NorESM2-EC (i.e.,
 81 NorESM with elevation classes to downscale the SMB within the model) compared to a dynamically
 82 downscaled SMB with the regional model MAR (NorESM2-MAR, Fettweis et al., 2017). This is further
 83 compared to the SMB as obtained by MAR when forced by the ERA5-observational product for the same
 84 period (ERA5-MAR), which can be seen as our observation-based target. While NorESM2 by itself
 85 (NorESM2-EC) captures the main features (north-south gradient, high SMB in the south-east, negative
 86 SMB in the central west), the dynamically downscaled products show considerably more detail and larger
 87 areas of negative SMB around the margins. Strong similarity between the two MAR products indicates
 88 that the dynamical downscaling has a larger impact on the results than the global boundary condition
 89 (NorESM2-MAR vs ERA5-MAR).

90

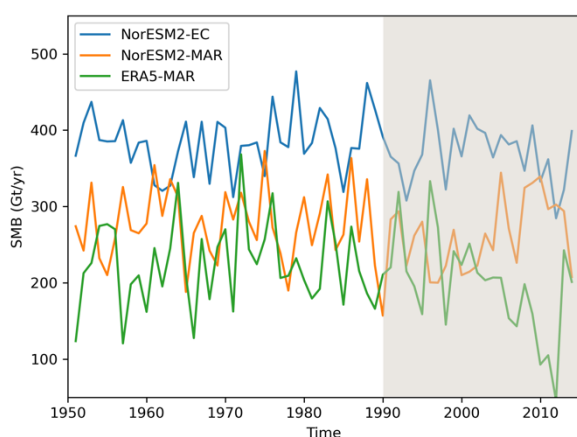


91
 92
 93

Figure 4 Mean surface mass balance (SMB) over the period 1960-1989 from a) NorESM2-EC, b) NorESM2-MAR and c) ERA5-MAR and differences (d-f). All three fields are masked to the modelled ice sheet area in NorESM2 at the end of year 2014.



94 Comparing the mean 1960-1989 SMB of NorESM2 with dynamically downscaled products NorESM2-
 95 MAR and ERA5-MAR shows that precipitation is smoothed out into the interior in the south-east, and
 96 topographically driven precipitation is generally not well resolved due to the relatively coarse resolution
 97 of the atmosphere model. A comparison with NorESM2-LM with a 2° horizontal resolution in the
 98 atmosphere illustrates these biases further (see supplementary Fig. S1). SMB around the margins is
 99 generally too high, which can partly be explained by a cold bias of the simulated near-surface
 00 temperatures over GrIS margins (cf. Seland et al., 2020). This is supported by the difference between
 01 NorESM2-MAR and ERA5-MAR, indicating that even after downscaling the SMB is biased high in
 02 NorESM2-MAR compared to the reanalysis-driven run.
 03



04
 05 **Figure 5 Historical total surface mass balance (SMB) variations integrated over the modelled ice sheet area.**

06 Due to the biases described above, the spatially integrated SMB is higher in NorESM2 (380 Gt/yr)
 07 compared to both NorESM2-MAR (284 Gt/yr) and ERA5-MAR (230 Gt/yr) (Fig. 5). Comparison
 08 between NorESM2-EC and NorESM2-MAR shows that the NorESM2 version used for downscaling with
 09 MAR is a different ensemble member with a different inter-annual and inter-decadal variability. This
 10 illustrates that direct comparison on inter-annual and even multi-decadal time scales of individual
 11 ensemble members with observations is problematic. That also applies to SMB trends after 1990 that are
 12 negative in NorESM2-EC and seemingly of the right sign when compared with ERA5-MAR, albeit with
 13 a muted response (-1.2 Gt/yr vs. -5.3 Gt/yr). Comparison with NorESM2-MAR with a positive SMB trend
 14 (4.0 Gt/yr) however clearly shows that the inter-annual/ inter-decadal variability in the ESM is not aligned
 15 with observations/reanalysis and can have considerable mismatch over these time intervals. The SMB
 16 trends after 2000 show increasing amplitude (both positive and negative) with -6.1 (7.9) [-8.9 Gt/yr] for
 17 NorESM2 (NorESM2-MAR) [ERA5-MAR].

18 The SMB variance over the period 1960-1989 in NorESM2 (1750 Gt/yr) is lower compared to NorESM2-
 19 MAR (2185 Gt/yr) and much lower compared to ERA5-MAR (2915 Gt/yr), which we attribute to an
 20 under-developed ablation area in NorESM2 that prohibits inter-annual temperature variations to fully
 21 translate to variations in melt and runoff. The Greenland cold bias in NorESM2 can explain the difference
 22 in variance between NorESM2-MAR and ERA5-MAR in a similar way.



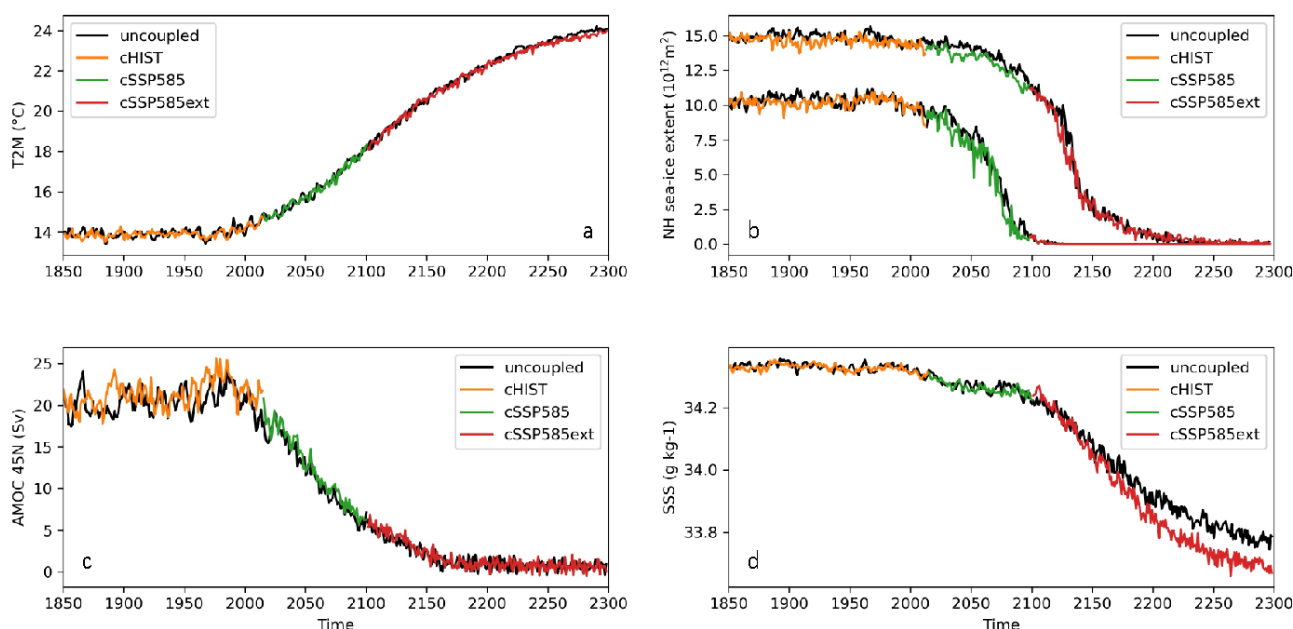
23

24 **4.2 Future projection**

25 Global mean temperature increases by ~ 3.5 °C between 2014 and 2100 and by ~ 10 °C in 2300 under
 26 SSP5-8.5 and extended forcing (Fig. 6a). Northern Hemisphere sea-ice extent dramatically decreases as
 27 a result (Fig. 6b), with the minimum extent reaching zero (sea-ice free summer Arctic) by the beginning
 28 of the 22st century and a maximum extent approaching zero by the beginning of the 23rd century
 29 (practically sea-ice free Arctic year-round). The Atlantic Meridional Overturning Circulation (AMOC)
 30 shows a decline already at the end of the historical experiment, which continues over the 21st and 22nd
 31 century to a near complete shutdown state at the end of the 23rd century (Fig. 6c).

32 Most global climate characteristics show similar behaviour in the coupled and uncoupled experiments,
 33 indicating that the interactive ice sheet coupling has limited effect on the large-scale climate behaviour in
 34 our model under the given forcing. In particular, the evolution of the AMOC is hardly affected by the
 35 additional freshwater flux from GrIS mass loss in the coupled experiment (cf. Figure 7a and b), which
 36 amounts to 0.004 Sv, 0.052 Sv and 0.113 Sv averaged over the 21st, 22nd and 23rd century, respectively.
 37 The only global variable where differences are clearly visible is global sea surface salinity that is reduced
 38 in the coupled model compared to NorESM2fixed (Fig. 6d) in response to that additional freshwater input.
 39 A detailed analysis of the (regional) differences between the coupled NorESM2 and the version with fixed
 40 ice sheets NorESM2fixed can be found in Haubner et al. (in prep).

41

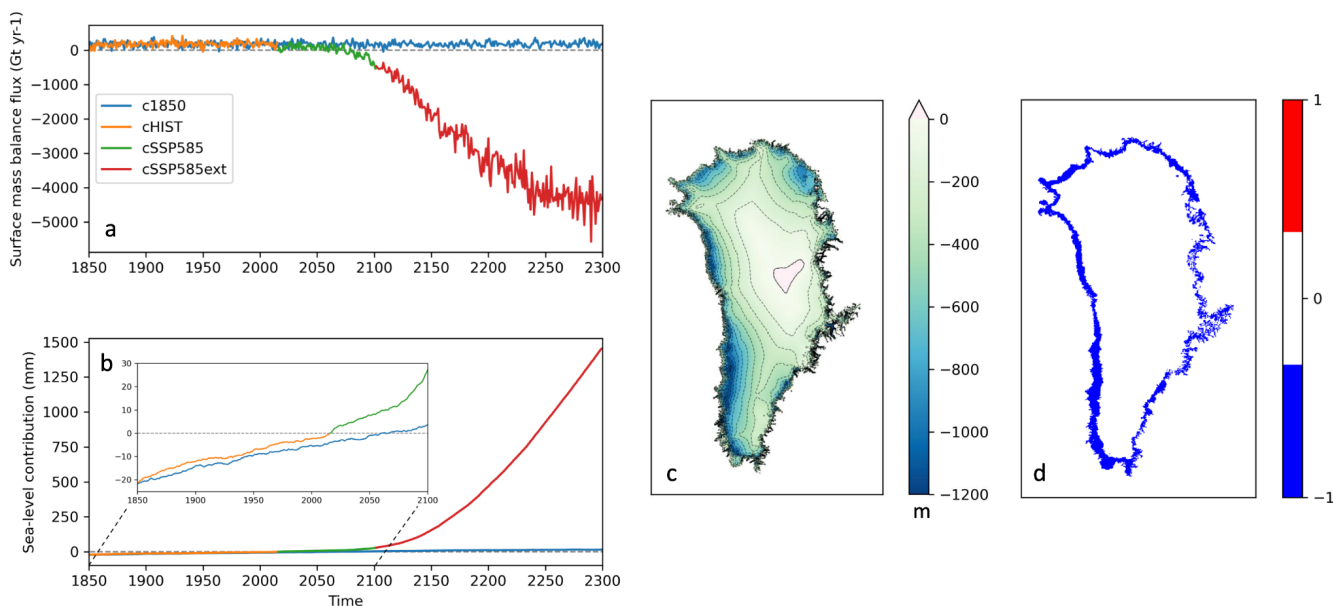


42
 43
 44

Figure 6 Large-scale climate characteristics for NorESM2 (colour) compared to NorESM2fixed (black). a) 2-m air temperature, b) maximum and minimum northern hemisphere sea-ice extent, c) AMOC strength at 45°N, d) sea surface salinity.



45 Increased mass loss of the GrIS compared to the historical background trend first emerges at the beginning
 46 of the projection period ~2015-2025 (Fig. 7b). However, instead of further accelerating ice sheet retreat
 47 after 2025, as might be expected from the global temperature evolution, we see a nearly constant rate of
 48 mass loss until 2080. This can be explained by a rapidly weakening AMOC, which leads to regional
 49 cooling in the North Atlantic that offsets a substantial part of the warming trend. Compared to results
 50 based on standalone ice sheet simulations over the same period with a large range of models (Goelzer et
 51 al., 2020), the projected sea-level contribution in NorESM2 is below the lower bound, which we attribute
 52 to both the strong AMOC response and an initial cold bias of NorESM2. However, a similar experiment
 53 with CESM2-CISM (Muntjewerf et al., 2020b) shows a strongly decreasing SMB already after 2050,
 54 despite a decreasing AMOC, which may be explained by a different ocean model or different interdecadal
 55 variability between the two global models.
 56 Mass loss rate increases towards the end of the 21st century and continues to do so until the end of our
 57 experiment in year 2300. The surface mass balance over the extension period is rapidly decreasing and
 58 leads to a cumulated sea-level contribution of close to 1.5 m by 2300 (Figure 7a-b). The ice sheet loses
 59 mass, thins by more than 1 km mainly around the coast, and exhibits retreat of several tens of km
 60 the entire margin (Figure 7c-d).
 61



62
 63 **Figure 7** GrIS characteristics for the chain of experiments: a) total surface mass balance, b) sea-level contribution, c) ice thickness
 64 change and d) ice mask change between 2014 and 2300 (blue indicating retreat).

65



66 **5 Discussion**

67 The presented model development and experiments represent the first interactive coupling of the GrIS in
68 the global Earth System Model NorESM. This work shines light on challenges that are inherent to
69 combining model components of different spatial resolution.

70 Climate model biases due to limited resolution of the atmospheric component are difficult to overcome,
71 given that current global climate models are typically run at the upper limit of available High Performance
72 Computing resources. While the elevation-class approach for downscaling is successful for SMB and
73 surface energy components with strong temperature dependence, improving the distribution of mostly
74 topographically controlled precipitation is very difficult. In this context, the potential of regional grid
75 refinement is promising, a possibility that emerges with the CAM spectral element dynamical core (Van
76 Kampenhout et al., 2019; Herrington et al., 2022) that will be available in future versions of NorESM.

77 NorESM2 has been initialised and run with a dynamic GrIS in a complementary way compared to the
78 approach taken with CESM2 (Muntjewerf et al., 2020a; b). Compared to these studies, we have tried to
79 initialise closer to observed ice sheet geometry and mitigate model drift by using stronger constraints on
80 the ice sheet model. The approach of nudging the ice sheet thickness toward observed values during
81 initialisation by calibrating the basal friction parameters is very effective but also has its caveats.
82 Inaccuracies in model physics, parametrisations and boundary conditions are compounded into a modified
83 basal friction field with effects that are hard to trace. In particular, any bias in the SMB (which we know
84 can be substantial in some regions) is propagated into the dynamic behaviour of the ice sheet model in a
85 non-transparent way (Berends et al. 2023). Masking the ice sheet to the observed present-day ice extent
86 is also a strong limitation to the ice sheet physics and is only justified for the strong warming scenario
87 applied here, where the entire ice sheet margin retreats. It remains a challenge to reduce the impact of
88 climate and ice sheet biases (which are often mutually reinforcing) on the coupled state while maintaining
89 the full prognostic capabilities of the model.

90 The assumption that the pre-industrial ice sheet state is close to the present-day observed one is
91 questionable and could be refined e.g. by running one or several iterations from pre-industrial to 1990
92 with an updated 1850 state to better match the transient historical ice sheet state. However, such a
93 refinement would add many more model years to the experimental setup, and its success could be
94 dependent on controlling internal variability of the system. Reconstructions of the climate and ice sheet
95 states further back in time, ideally towards the pre-industrial climate, would be very useful in this context.
96 Since we have focused on describing the ice sheet coupling, we have not analysed the climate evolution
97 over the historical and future period in great detail. A deeper analysis of differences between the coupled
98 and uncoupled experiments can be found in a separate paper (Haubner et al., in prep). However, it is
99 apparent that the influence of ice sheet changes on the global mean climate is rather limited in the current
00 setup and for the given forcing. In particular, we may have expected a larger response of the AMOC to
01 the additional freshwater input coming from Greenland, even if the lack of a dedicated ocean forcing in
02 our setup may be under-estimating ice sheet retreat to some extent. It appears that the AMOC weakening
03 in the model version without ice sheet coupling is already so intense in NorESM2 (Schwinger et al.,
04 2022), that the freshening due to ice sheet meltwater fluxes has little additional effect.



05 **6 Conclusions**

06 This paper describes the first coupled climate–Greenland ice sheet model setup of NorESM and illustrates
07 its behaviour with first simulation results. We have presented modelling choices which are effective in
08 working around some of the climate biases and in preparing a present-day ice sheet state that is close to
09 observations. The simulated present-day surface mass balance in NorESM captures the main features
10 when compared to high-fidelity regional climate model simulations but does not represent the detailed
11 distribution of precipitation very well due to the relatively coarse resolution of the atmosphere.
12 Experiments under a strong future warming scenario until 2300 show a limited effect of including the
13 Greenland coupling on most global variables under the given forcing.

14 Other challenges of coupling Earth system components of different typical response timescales and spatial
15 resolution remain. Further work with NorESM is therefore ongoing e.g. to include the coupling of marine-
16 terminating outlet glaciers with the ocean, and to improve the representation of SMB over the GrIS. We
17 are also working towards coupling with the Antarctic ice sheet, which is an obvious next step but includes
18 additional challenges, in particular a less effective downscaling of SMB boundary conditions due to a
19 limited contribution of melt and the important interaction between ice shelves and the Southern Ocean.

20 **Code and data availability**

21 The NorESM model code is developed and freely available under
22 <https://github.com/NorESMhub/NorESM>. The specific code repository used to set up the model is
23 archived under <https://doi.org/10.5281/zenodo.11199967>. The full code used to produce the coupled
24 experiments is persistently archived under <https://doi.org/10.5281/zenodo.11200059>.

25 The raw data for the coupled NorESM2 experiments has been archived with persistent identifiers
26 <https://doi.org/10.11582/2024.00079>, <https://doi.org/10.11582/2024.00080>,
27 <https://doi.org/10.11582/2024.00081> and <https://doi.org/10.11582/2024.00082>. The CMORized output
28 from the NorESM2fixed experiments (Bentsen et al., 2019a;b) can be accessed through the ESGF at
29 <https://doi.org/10.22033/ESGF/CMIP6.8040> and <https://doi.org/10.22033/ESGF/CMIP6.8321>.

30 **Author contributions**

31 HG, PML and AB designed the experimental setup. HG developed the Greenland coupling with help of
32 PML, AB, WHL, GL and KTC. HG conducted the coupled NorESM experiments and wrote the
33 manuscript with help from all co-authors.

34 **Competing interests**

35 The contact author has declared that none of the authors has any competing interests.



36 **Disclaimer**

37 Publisher's note: Copernicus Publications remains neutral with regard to jurisdictional claims made in the
38 text, published maps, institutional affiliations, or any other geographical representation in this paper.
39 While Copernicus Publications makes every effort to include appropriate place names, the final
40 responsibility lies with the authors.

41 **Acknowledgements**

42 We thank Michael Schulz, Mats Bentsen, Trude Storelvmo and all the other KeyCLIM and INES project
43 participants for discussions and suggestions that supported the model development and analysis of the
44 simulations. We thank the Norwegian Climate Centre for providing NorESM2 data for CMIP6 and the
45 Earth System Grid Federation (ESGF) for archiving the CMIP data and providing access. High-
46 performance computing and storage resources were provided by Sigma2 - the National Infrastructure for
47 High Performance Computing and Data Storage in Norway through projects NN9560K, NN9252K,
48 NN2345K, NN8006K, NS9560K, NS9252K, NS2345K, NS9034K and NS8006K.

49 **Financial support**

50 This research has been supported by the Research Council of Norway under projects KeyClim (295046),
51 INES (270061) and GREASE (324639). GL, WHL, and KTC are supported by the NSF National Center
52 for Atmospheric Research, which is a major facility sponsored by the National Science Foundation under
53 Cooperative Agreement no. 1852977.

54 **References**

- 55 Bentsen, M., Oliviè, D. J. L., Seland, Ø., Toniazzo, T., Gjermundsen, A., Graff, L. S., Debernard, J. B., Gupta, A.
56 K., He, Y., Kirkevåg, A., Schwinger, J., Tjiputra, J., Aas, K. S., Bethke, I., Fan, Y., Griesfeller, J., Grini, A.,
57 Guo, C., Ilicak, M., Karset, I. H. H., Landgren, O. A., Liakka, J., Moseid, K. O., Nummelin, A.,
58 Spensberger, C., Tang, H., Zhang, Z., Heinze, C., Iversen, T., and Schulz, M.: NCC NorESM2-MM model
59 output prepared for CMIP6 CMIP historical, <https://doi.org/10.22033/ESGF/CMIP6.8040>, 2019a.
- 60 Bentsen, M., Oliviè, D. J. L., Seland, Ø., Toniazzo, T., Gjermundsen, A., Graff, L. S., Debernard, J. B., Gupta, A.
61 K., He, Y., Kirkevåg, A., Schwinger, J., Tjiputra, J., Aas, K. S., Bethke, I., Fan, Y., Griesfeller, J., Grini, A.,
62 Guo, C., Ilicak, M., Karset, I. H. H., Landgren, O. A., Liakka, J., Moseid, K. O., Nummelin, A.,
63 Spensberger, C., Tang, H., Zhang, Z., Heinze, C., Iversen, T., and Schulz, M.: NCC NorESM2-MM model
64 output prepared for CMIP6 ScenarioMIP ssp585, <https://doi.org/10.22033/ESGF/CMIP6.8321>, 2019b.
- 65 Berdahl, M., Leguy, G., Lipscomb, W. H., Urban, N. M., and Hoffman, M. J.: Exploring ice sheet model
66 sensitivity to ocean thermal forcing and basal sliding using the Community Ice Sheet Model (CISM), *The*
67 *Cryosphere*, 17, 1513–1543, <https://doi.org/10.5194/tc-17-1513-2023>, 2023.



- 68 Berends, C. J., Van De Wal, R. S. W., Van Den Akker, T., and Lipscomb, W. H.: Compensating errors in
69 inversions for subglacial bed roughness: same steady state, different dynamic response, *Cryosphere*, 17,
70 1585–1600, <https://doi.org/10.5194/tc-17-1585-2023>, 2023.
- 71 Bjørk, A. A., Kjær, K. H., Korsgaard, N. J., Khan, S. A., Kjeldsen, K. K., Andresen, C. S., Larsen, N. K., and
72 Funder, S.: An aerial view of 80 years of climate-related glacier fluctuations in southeast Greenland, *Nature*
73 *Geoscience*, 5, 427–432, <https://doi.org/10.1038/ngeo1481>, 2012.
- 74 Box, J. E. and Colgan, W.: Greenland ice sheet mass balance reconstruction. Part III: Marine ice loss and total
75 mass balance (1840–2010), *Journal of Climate*, 26, 6990–7002, <https://doi.org/10.1175/JCLI-D-12-00546.1>,
76 2013.
- 77 Danabasoglu, G., Lamarque, J.-F., Bacmeister, J., Bailey, D. A., DuVivier, A. K., Edwards, J., Emmons, L. K.,
78 Fasullo, J., Garcia, R., Gettelman, A., Hannay, C., Holland, M. M., Large, W. G., Lauritzen, P. H.,
79 Lawrence, D. M., Lenaerts, J. T. M., Lindsay, K., Lipscomb, W. H., Mills, M. J., Neale, R., Oleson, K. W.,
80 Otto-Bliessner, B., Phillips, A. S., Sacks, W., Tilmes, S., van Kampenhout, L., Vertenstein, M., Bertini, A.,
81 Dennis, J., Deser, C., Fischer, C., Fox-Kemper, B., Kay, J. E., Kinnison, D., Kushner, P. J., Larson, V. E.,
82 Long, M. C., Mickelson, S., Moore, J. K., Nienhouse, E., Polvani, L., Rasch, P. J., and Strand, W. G.: The
83 Community Earth System Model Version 2 (CESM2), *Journal of Advances in Modeling Earth Systems*, 12,
84 e2019MS001916–e2019MS001916, <https://doi.org/10.1029/2019MS001916>, 2020.
- 85 Eyring, V., Bony, S., Meehl, G. A., Senior, C. A., Stevens, B., Stouffer, R. J., and Taylor, K. E.: Overview of the
86 Coupled Model Intercomparison Project Phase 6 (CMIP6) experimental design and organization,
87 *Geoscientific Model Development*, 9, 1937–1958, <https://doi.org/10.5194/gmd-9-1937-2016>, 2016.
- 88 Fettweis, X., Box, J. E., Agosta, C., Amory, C., Kittel, C., Lang, C., van As, D., Machguth, H., and Gallée, H.:
89 Reconstructions of the 1900–2015 Greenland ice sheet surface mass balance using the regional climate
90 MAR model, *The Cryosphere*, 11, 1015–1015, <https://doi.org/10.5194/tc-11-1015-2017>, 2017.
- 91 Fyke, J. G., Sacks, W. J., and Lipscomb, W. H.: A technique for generating consistent ice sheet initial conditions
92 for coupled ice sheet/climate models, *Geoscientific Model Development*, 7, 1183–1195,
93 <https://doi.org/10.5194/gmd-7-1183-2014>, 2014.
- 94 Ganopolski, A., Calov, R., and Claussen, M.: Simulation of the last glacial cycle with a coupled climate ice-sheet
95 model of intermediate complexity, *Climate of the Past*, 6, 229–244, <https://doi.org/10.5194/cp-6-229-2010>,
96 2010.
- 97 Goelzer, H., Huybrechts, P., Loutre, M. F., Goosse, H., Fichefet, T., and Mouchet, A.: Impact of Greenland and
98 Antarctic ice sheet interactions on climate sensitivity, *Climate Dynamics*, 37, 1005–1018,
99 <https://doi.org/10.1007/s00382-010-0885-0>, 2011.
- 00 Goelzer, H., Huybrechts, P., Raper, S. C. B., Loutre, M. F., Goosse, H., and Fichefet, T.: Millennial total sea-
01 level commitments projected with the Earth system model of intermediate complexity LOVECLIM,
02 *Environmental Research Letters*, 7, 045401, <https://doi.org/10.1088/1748-9326/7/4/045401>, 2012.
- 03 Goelzer, H., Nowicki, S., Payne, A., Larour, E., Seroussi, H., Lipscomb, W. H., Gregory, J., Abe-Ouchi, A.,
04 Shepherd, A., Simon, E., Agosta, C., Alexander, P., Aschwanden, A., Barthel, A., Calov, R., Chambers, C.,
05 Choi, Y., Cuzzone, J., Dumas, C., Edwards, T., Felikson, D., Fettweis, X., Gollledge, N. R., Greve, R.,
06 Humbert, A., Huybrechts, P., Le clec’h, S., Lee, V., Leguy, G., Little, C., Lowry, D. P., Morlighem, M.,
07 Nias, I., Quiquet, A., Rückamp, M., Schlegel, N.-J., Slater, D. A., Smith, R. S., Straneo, F., Tarasov, L., van
08 de Wal, R., and van den Broeke, M.: The future sea-level contribution of the Greenland ice sheet: a multi-
09 model ensemble study of ISMIP6, *The Cryosphere*, 14, 3071–3096, [https://doi.org/10.5194/tc-14-3071-](https://doi.org/10.5194/tc-14-3071-2020)
10 [2020](https://doi.org/10.5194/tc-14-3071-2020), 2020.



- 11 Goldberg, D. N.: A variationally derived, depth-integrated approximation to a higher-order glaciological flow
12 model, *Journal of Glaciology*, 57, 157–170, <https://doi.org/10.3189/002214311795306763>, 2011.
- 13 Gregory, J. M., George, S. E., and Smith, R. S.: Large and irreversible future decline of the Greenland ice sheet,
14 *Cryosphere*, 14, 4299–4322, <https://doi.org/10.5194/tc-14-4299-2020>, 2020.
- 15 Haubner, K., Goelzer, Heiko, and Born, Andreas: Limited global effect of climate-Greenland ice sheet
16 coupling in NorESM under a high-emission scenario, in prep.
- 17 Hermann, M., Box, J. E., Fausto, R. S., Colgan, W. T., Langen, P. L., Mottram, R., Wuite, J., Noël, B., van den
18 Broeke, M. R., and van As, D.: Application of PROMICE Q-Transect in Situ Accumulation and Ablation
19 Measurements (2000–2017) to Constrain Mass Balance at the Southern Tip of the Greenland Ice Sheet,
20 *Journal of Geophysical Research: Earth Surface*, 123, 1235–1256, <https://doi.org/10.1029/2017JF004408>,
21 2018.
- 22 Herrington, A. R., Lauritzen, P. H., Lofverstrom, M., Lipscomb, W. H., Gettelman, A., and Taylor, M. A.: Impact
23 of Grids and Dynamical Cores in CESM2.2 on the Surface Mass Balance of the Greenland Ice Sheet,
24 *Journal of Advances in Modeling Earth Systems*, 14, e2022MS003192,
25 <https://doi.org/10.1029/2022MS003192>, 2022.
- 26 Huybrechts, P., Janssens, I., Poncin, C., and Fichefet, T.: The response of the Greenland ice sheet to climate
27 changes in the 21st century by interactive coupling of an AOGCM with a thermomechanical ice-sheet
28 model, *Annals of Glaciology*, 35, 409–415, <https://doi.org/10.3189/172756402781816537>, 2002.
- 29 Lawrence, D. M., Fisher, R. A., Koven, C. D., Oleson, K. W., Swenson, S. C., Bonan, G., Collier, N., Ghimire,
30 B., van Kampenhout, L., Kennedy, D., Kluzek, E., Lawrence, P. J., Li, F., Li, H., Lombardozzi, D., Riley,
31 W. J., Sacks, W. J., Shi, M., Vertenstein, M., Wieder, W. R., Xu, C., Ali, A. A., Badger, A. M., Bisht, G.,
32 van den Broeke, M., Brunke, M. A., Burns, S. P., Buzan, J., Clark, M., Craig, A., Dahlin, K., Drewniak, B.,
33 Fisher, J. B., Flanner, M., Fox, A. M., Gentine, P., Hoffman, F., Keppel-Aleks, G., Knox, R., Kumar, S.,
34 Lenaerts, J., Leung, L. R., Lipscomb, W. H., Lu, Y., Pandey, A., Pelletier, J. D., Perket, J., Randerson, J. T.,
35 Ricciuto, D. M., Sanderson, B. M., Slater, A., Subin, Z. M., Tang, J., Thomas, R. Q., Val Martin, M., and
36 Zeng, X.: The Community Land Model Version 5: Description of New Features, Benchmarking, and Impact
37 of Forcing Uncertainty, *Journal of Advances in Modeling Earth Systems*, 11, 4245–4287,
38 <https://doi.org/10.1029/2018MS001583>, 2019.
- 39 Lipscomb, W. H., Fyke, J. G., Vizcaíno, M., Sacks, W. J., Wolfe, J., Vertenstein, M., Craig, A., Kluzek, E., and
40 Lawrence, D. M.: Implementation and initial evaluation of the glimmer community ice sheet model in the
41 community earth system model, *Journal of Climate*, 26, 7352–7371, <https://doi.org/10.1175/JCLI-D-12-00557.1>, 2013.
- 43 Lipscomb, W. H., Price, S. F., Hoffman, M. J., Leguy, G. R., Bennett, A. R., Bradley, S. L., Evans, K. J., Fyke, J.
44 G., Kennedy, J. H., Perego, M., Ranken, D. M., Sacks, W. J., Salinger, A. G., Vargo, L. J., and Worley, P.
45 H.: Description and evaluation of the Community Ice Sheet Model (CISM) v2.1, *Geoscientific Model
46 Development*, 12, 387–424, <https://doi.org/10.5194/gmd-12-387-2019>, 2019.
- 47 Lipscomb, W. H., Leguy, G. R., Jourdain, N. C., Asay-Davis, X., Seroussi, H., and Nowicki, S.: ISMIP6-based
48 projections of ocean-forced Antarctic Ice Sheet evolution using the Community Ice Sheet Model,
49 *Cryosphere*, 15, 633–661, <https://doi.org/10.5194/tc-15-633-2021>, 2021.
- 50 Lofverstrom, M., Fyke, J. G., Thayer-Calder, K., Muntjewerf, L., Vizcaino, M., Sacks, W. J., Lipscomb, W. H.,
51 Otto-Bliesner, B. L., and Bradley, S. L.: An Efficient Ice Sheet/Earth System Model Spin-up Procedure for
52 CESM2-CISM2: Description, Evaluation, and Broader Applicability, *Journal of Advances in Modeling
53 Earth Systems*, 12, e2019MS001984, <https://doi.org/10.1029/2019MS001984>, 2020.



- 54 Martin, T. and Biastoch, A.: On the ocean's response to enhanced Greenland runoff in model experiments:
55 relevance of mesoscale dynamics and atmospheric coupling, *Ocean Sci.*, 19, 141–167,
56 <https://doi.org/10.5194/os-19-141-2023>, 2023.
- 57 Merz, N., Gfeller, G., Born, A., Raible, C. C., Stocker, T. F., and Fischer, H.: Influence of ice sheet
58 topography on Greenland precipitation during the Eemian interglacial, *Journal of Geophysical Research*,
59 119, 10,749–10,768, <https://doi.org/10.1002/2014JD021940>, 2014.
- 60 Merz, N., Born, A., Raible, C. C., and Stocker, T. F.: Warm Greenland during the last interglacial: the role
61 of regional changes in sea ice cover, *Clim. Past*, 12, 2011–2031, <https://doi.org/10.5194/cp-12-2011-2016>,
62 2016.
- 63 Mikolajewicz, U., Vizcaino, M., JungCLAUS, J., and Schurgers, G.: Effect of ice sheet interactions in
64 anthropogenic climate change simulations, *Geophysical Research Letters*, 34, 5,
65 <https://doi.org/10.1029/2007gl031173>, 2007.
- 66 Muntjewerf, L., Sellevold, R., Vizcaino, M., Ernani da Silva, C., Petrini, M., Thayer-Calder, K., Scherrenberg,
67 M. D. W., Bradley, S. L., Katsman, C. A., Fyke, J., Lipscomb, W. H., Lofverstrom, M., and Sacks, W. J.:
68 Accelerated Greenland Ice Sheet Mass Loss Under High Greenhouse Gas Forcing as Simulated by the
69 Coupled CESM2.1-CISM2.1, *Journal of Advances in Modeling Earth Systems*, 12, 1–21,
70 <https://doi.org/10.1029/2019MS002031>, 2020a.
- 71 Muntjewerf, L., Petrini, M., Vizcaino, M., Ernani da Silva, C., Sellevold, R., Scherrenberg, M. D. W., Thayer-
72 Calder, K., Bradley, S. L., Lenaerts, J. T. M., Lipscomb, W. H., and Lofverstrom, M.: Greenland Ice Sheet
73 Contribution to 21st Century Sea Level Rise as Simulated by the Coupled CESM2.1-CISM2.1, *Geophysical
74 Research Letters*, 47, <https://doi.org/10.1029/2019GL086836>, 2020b.
- 75 Muntjewerf, L., Sacks, W. J., Lofverstrom, M., Fyke, J., Lipscomb, W. H., Ernani da Silva, C., Vizcaino, M.,
76 Thayer-Calder, K., Lenaerts, J. T. M., and Sellevold, R.: Description and Demonstration of the Coupled
77 Community Earth System Model v2 – Community Ice Sheet Model v2 (CESM2-CISM2), *Journal of
78 Advances in Modeling Earth Systems*, 13, e2020MS002356, <https://doi.org/10.1029/2020MS002356>, 2021.
- 79 Nowicki, S. M. J., Payne, A., Larour, E., Seroussi, H., Goelzer, H., Lipscomb, W., Gregory, J., Abe-Ouchi, A.,
80 and Shepherd, A.: Ice Sheet Model Intercomparison Project (ISMIP6) contribution to CMIP6, *Geoscientific
81 Model Development*, 9, 4521–4545, <https://doi.org/10.5194/gmd-9-4521-2016>, 2016.
- 82 O'Neill, B. C., Tebaldi, C., van Vuuren, D. P., Eyring, V., Friedlingstein, P., Hurtt, G., Knutti, R., Kriegler, E.,
83 Lamarque, J.-F., Lowe, J., Meehl, G. A., Moss, R., Riahi, K., and Sanderson, B. M.: The Scenario Model
84 Intercomparison Project (ScenarioMIP) for CMIP6, *Geosci. Model Dev.*, 9, 3461–3482,
85 <https://doi.org/10.5194/gmd-9-3461-2016>, 2016.
- 86 Pattyn, F., Ritz, C., Hanna, E., Asay-Davis, X., DeConto, R., Durand, G., Favier, L., Fettweis, X., Goelzer, H.,
87 Golledge, N. R., Kuipers Munneke, P., Lenaerts, J. T. M., Nowicki, S., Payne, A. J., Robinson, A., Seroussi,
88 H., Trusel, L. D., and van den Broeke, M.: The Greenland and Antarctic ice sheets under 1.5 °C global
89 warming, *Nature Clim Change*, 8, 1053–1061, <https://doi.org/10.1038/s41558-018-0305-8>, 2018.
- 90 Petrini, M., Scherrenberg, M., Muntjewerf, L., Vizcaino, M., Sellevold, R., Leguy, G., Lipscomb, W., and
91 Goelzer, H.: A topographically-controlled tipping point for complete Greenland ice-sheet melt, *The
92 Cryosphere Discussions*, 1–28, <https://doi.org/10.5194/tc-2023-154>, 2023.
- 93 Rahlves, C., Goelzer, H., Born, A., and Langebroek, P. M.: Historically consistent mass loss projections of the
94 Greenland ice sheet, *EGUsphere*, 1–24, <https://doi.org/10.5194/egusphere-2024-922>, 2024.
- 95 Ridley, J. K., Huybrechts, P., Gregory, J. M., and Lowe, J. A.: Elimination of the Greenland Ice Sheet in a High
96 CO₂ Climate, *Journal of Climate*, 18, 3409–3427, <https://doi.org/10.1175/JCLI3482.1>, 2005.



- 97 Robinson, A., Goldberg, D., and Lipscomb, W. H.: A comparison of the stability and performance of depth-
98 integrated ice-dynamics solvers, *Cryosphere*, 16, 689–709, <https://doi.org/10.5194/tc-16-689-2022>, 2022.
- 99 Roche, D. M., Dumas, C., Bügelmayer, M., Charbit, S., and Ritz, C.: Adding a dynamical cryosphere to
100 iLOVECLIM (version 1.0): Coupling with the GRISLI ice-sheet model, *Geoscientific Model Development*,
101 7, 1377–1394, <https://doi.org/10.5194/gmd-7-1377-2014>, 2014.
- 102 Schoof, C.: The effect of cavitation on glacier sliding, *Proceedings of the Royal Society A: Mathematical,*
103 *Physical and Engineering Sciences*, 461, 609–627, <https://doi.org/10.1098/rspa.2004.1350>, 2005.
- 104 Schwinger, J., Asaadi, A., Goris, N., and Lee, H.: Possibility for strong northern hemisphere high-latitude cooling
105 under negative emissions, *Nature Communications*, 13, 1095, <https://doi.org/10.1038/s41467-022-28573-5>,
106 2022.
- 107 Seland, Ø., Bentsen, M., Olivié, D., Toniazzo, T., Gjermundsen, A., Graff, L. S., Debernard, J. B., Gupta, A. K.,
108 He, Y. C., Kirkevåg, A., Schwinger, J., Tjiputra, J., Schanke Aas, K., Bethke, I., Fan, Y., Griesfeller, J.,
109 Grini, A., Guo, C., Ilicak, M., Karset, I. H. H., Landgren, O., Liakka, J., Moseid, K. O., Nummelin, A.,
110 Spensberger, C., Tang, H., Zhang, Z., Heinze, C., Iversen, T., and Schulz, M.: Overview of the Norwegian
111 Earth System Model (NorESM2) and key climate response of CMIP6 DECK, historical, and scenario
112 simulations, 13, 6200, <https://doi.org/10.5194/gmd-13-6165-2020>, 2020.
- 113 Sellevold, R., van Kampenhout, L., Lenaerts, J. T. M., Noël, B., Lipscomb, W. H., and Vizcaino, M.: Surface
114 mass balance downscaling through elevation classes in an Earth system model: application to the Greenland
115 ice sheet, *The Cryosphere*, 13, 3193–3208, <https://doi.org/10.5194/tc-13-3193-2019>, 2019.
- 116 Seroussi, H., Nowicki, S., Payne, A. J., Goelzer, H., Lipscomb, W. H., Abe-Ouchi, A., Agosta, C. C.,
117 Albrecht, T., Asay-Davis, X., Barthel, A., Calov, R., Cullather, R., Dumas, C., Galton-Fenzi, B. K.,
118 Gladstone, R., Golledge, N. R., Gregory, J. M., Greve, R., Hattermann, T., Hoffman, M. J., Humbert, A.,
119 Huybrechts, P., Jourdain, N. C., Kleiner, T., Larour, E., Leguy, G. R., Lowry, D. P., Little, C. M.,
120 Morlighem, M., Pattyn, F., Pelle, T., Price, S. S. F., Quiquet, A. A., Reese, R., Schlegel, N.-J., Shepherd,
121 A., Simon, E., Smith, R. S., Straneo, F., Sun, S., Trusel, L. D., Van Breedam, J., van de Wal, R. S. W.,
122 Winkelmann, R., Zhao, C., Zhang, T., Zwinger, T., Ouchi, A. A., Agosta, C. C., Albrecht, T., Asay-Davis,
123 X., Barthel, A., Calov, R., Cullather, R., Dumas, C., Gladstone, R., Goelzer, H., Golledge, N. R., Gregory,
124 J. M., Greve, R., Hattermann, T., Hoffman, M. J., Huybrechts, P., Jourdain, N. C., Kleiner, T., Larour, E.,
125 Leguy, G. R., Lipscomb, W. H., Lowry, D. P., Little, C. M., Mengel, M., Morlighem, M., Pattyn, F., Payne,
126 A. J., Pelle, T., Price, S. S. F., Quiquet, A. A., Reese, R., Schlegel, N.-J., Shepherd, A., Simon, E., Smith, R.
127 S., Straneo, F., Sun, S., Trusel, L. D., Breedam, J. V., Wal, R. S. W. van de, Winkelmann, R., Zhao, C.,
128 Zhang, T., Goelzer, H., Lipscomb, W. H., Abe-Ouchi, A., Agosta, C. C., Albrecht, T., Asay-Davis, X.,
129 Barthel, A., Calov, R., Cullather, R., et al.: ISMIP6 Antarctica: a multi-model ensemble of the Antarctic ice
130 sheet evolution over the 21st century, *The Cryosphere*, 14, 3033–3070, [https://doi.org/10.5194/tc-14-3033-](https://doi.org/10.5194/tc-14-3033-2020)
131 2020, 2020.
- 132 Seroussi, H., Pelle, T., Lipscomb, W. H., Abe-Ouchi, A., Albrecht, T., Alvarez-Solas, J., Asay-Davis, X.,
133 Barre, J.-B., Berends, C. J., Bernales, J., Blasco, J., Caillet, J., Chandler, D. M., Coulon, V., Cullather, R.,
134 Dumas, C., Galton-Fenzi, B. K., Garbe, J., Gillet-Chaulet, F., Gladstone, R., Goelzer, H., Golledge, N.,
135 Greve, R., Gudmundsson, G. H., Han, H. K., Hillebrand, T. R., Hoffman, M. J., Huybrechts, P., Jourdain,
136 N. C., Klose, A. K., Langebroek, P. M., Leguy, G. R., Lowry, D. P., Mathiot, P., Montoya, M., Morlighem,
137 M., Nowicki, S., Pattyn, F., Payne, A. J., Quiquet, A., Reese, R., Robinson, A., Saraste, L., Simon, E. G.,
138 Sun, S., Twarog, J. P., Trusel, L. D., Urruty, B., Van Breedam, J., van de Wal, R. S. W., Wang, Y., Zhao,
139 C., and Zwinger, T.: Evolution of the Antarctic Ice Sheet Over the Next Three Centuries From an ISMIP6
140 Model Ensemble, *Earth's Future*, 12, e2024EF004561, <https://doi.org/10.1029/2024EF004561>, 2024.



- 41 Slater, D. A., Straneo, F., Felikson, D., Little, C. M., Goelzer, H., Fettweis, X., and Holte, J.: Estimating
42 Greenland tidewater glacier retreat driven by submarine melting, *The Cryosphere*, 13, 2489–2509,
43 <https://doi.org/10.5194/tc-13-2489-2019>, 2019.
- 44 Slater, D. A., Felikson, D., Straneo, F., Goelzer, H., Little, C. M., Morlighem, M., Fettweis, X., and Nowicki, S.:
45 Twenty-first century ocean forcing of the Greenland ice sheet for modelling of sea level contribution, *The*
46 *Cryosphere*, 14, 985–1008, <https://doi.org/10.5194/tc-14-985-2020>, 2020.
- 47 Smith, R. S., Mathiot, P., Siahaan, A., Lee, V., Cornford, S. L., Gregory, J. M., Payne, A. J., Jenkins, A.,
48 Holland, P. R., Ridley, J. K., and Jones, C. G.: Coupling the U.K. Earth System Model to Dynamic Models
49 of the Greenland and Antarctic Ice Sheets, *Journal of Advances in Modeling Earth Systems*, 13,
50 e2021MS002520, <https://doi.org/10.1029/2021MS002520>, 2021.
- 51 Stone, E. J. and Lunt, D. J.: The role of vegetation feedbacks on Greenland glaciation, *Climate Dynamics*, 40,
52 2671–2686, <https://doi.org/10.1007/s00382-012-1390-4>, 2013.
- 53 van de Wal, R. S. W., Boot, W., Smeets, C. J. P. P., Snellen, H., van den Broeke, M. R., and Oerlemans, J.:
54 Twenty-one years of mass balance observations along the K-transect, West Greenland, *Earth Syst. Sci.*
55 *Data*, 4, 31–35, <https://doi.org/10.5194/essd-4-31-2012>, 2012.
- 56 Van Kampenhout, L., Rhoades, A. M., Herrington, A. R., Zarzycki, C. M., Lenaerts, J. T. M., Sacks, W. J., and
57 Van Den Broeke, M. R.: Regional grid refinement in an Earth system model: Impacts on the simulated
58 Greenland surface mass balance, *Cryosphere*, 13, 1547–1564, <https://doi.org/10.5194/tc-13-1547-2019>,
59 2019.
- 60 Vizcaino, M.: Ice sheets as interactive components of Earth System Models: progress and challenges, *WIREs*
61 *Climate Change*, 5, 557–568, <https://doi.org/10.1002/wcc.285>, 2014.
- 62 Vizcaíno, M., Mikolajewicz, U., Jungclaus, J., Schurgers, G., Vizcaino, M., Mikolajewicz, U., Jungclaus, J.,
63 Schurgers, G., Vizcaíno, M., Mikolajewicz, U., Jungclaus, J., and Schurgers, G.: Climate modification by
64 future ice sheet changes and consequences for ice sheet mass balance, *Climate Dynamics*, 34, 301–324,
65 <https://doi.org/10.1007/s00382-009-0591-y>, 2010.
- 66 Vizcaíno, M., Lipscomb, W. H., Sacks, W. J., Angelen, J. H. van, Wouters, B., Broeke, M. R. van den, Van
67 Angelen, J. H., Wouters, B., and Van Den Broeke, M. R.: Greenland surface mass balance as simulated by
68 the community earth system model. Part I: Model evaluation and 1850-2005 results, *Journal of Climate*, 26,
69 7793–7812, <https://doi.org/10.1175/JCLI-D-12-00615.1>, 2013.
- 70 Vizcaíno, M., Lipscomb, W. H., Sacks, W. J., and Broeke, M. van den: Greenland Surface Mass Balance as
71 Simulated by the Community Earth System Model. Part II: Twenty-First-Century Changes, *Journal of*
72 *Climate*, 27, 215–226, <https://doi.org/10.1175/JCLI-D-12-00588.1>, 2014.
- 73 Zuo, Z. and Oerlemans, J.: Contribution of glacier melt to sea-level rise since AD 1865: a regionally
74 differentiated calculation, *Climate Dynamics*, 13, 835–845, <https://doi.org/10.1007/s003820050200>, 1997.
- 75